J. Cent. South Univ. (2019) 26: 2318−2327
DOI: https://doi.org/10.1007/s11771-019-4176-6

Springer

Investigation of weld parameters on ductility, onion ring and fracture behaviour of friction stir welded AA2219-T87

Dinesh KUMAR R[1], S MUTHUKUMARAN[1], Vincent XAVIER[2], T VENKATESWARAN[2], D SIVAKUMAR[2]

1. Department of Metallurgical and Materials Engineering, NIT-Trichy 620015, India;
2. Heat Treatment and Welding Metallurgy Division, Vikram Sarabhai Space Centre (VSSC-ISRO), Trivandrum 695022, India

Abstract: Friction stir welding provides better retention of ductility and plasticity in comparison to fusion welding and it increases the stability against cracking. This study aims to enhance both the ductility and strength of the welded joints. Tool profile was found to play an important role in retaining ductility, understanding the metal flow behavior and determining the fracture initiating point. The microstructure of different regions in the onion ring was inferred to correlate the strength with the metal flow pattern. The onion ring pattern strengthened the weld nugget. Shoulder and taper threaded profile tool resulted in superior mechanical properties. Microhardness results confirmed that the fracture runs through low hardness areas such as heat affected zone and thermo-mechanically affected zone. The scanning electron microscopic images revealed elongated grains and dimples, justifying ductile mode of fracture.

Key words: plasticity; metal flow; onion ring; fracture; friction stir welding

Cite this article as: Dinesh KUMAR R, S MUTHUKUMARAN, Vincent XAVIER, T VENKATESWARAN, D SIVAKUMAR. Investigation of weld parameters on ductility, onion ring and fracture behaviour of friction stir welded AA2219-T87 [J]. Journal of Central South University, 2019, 26(9): 2318−2327. DOI: https://doi.org/10.1007/s11771-019-4176-6.

1 Introduction

Friction stir welding (FSW) is a solid-state welding process that works on the principle of plastic deformation of material [1]. Welding is done by plunging the tool pin into the workpiece until the tool shoulder comes in contact with the workpiece surface. A tool with unique features in pin and shoulder tends to exhibit better metal flow than normal profile [2]. The friction generated plasticizes and joins the material through two modes of metal transfer. Metal moved by the shoulder forms first mode and remaining metal moved by the pin generates second mode of metal transfer. The metal flow across the pin takes place either in retreating side or both retreating and advancing side [3].

AA2219 has excellent mechanical property through a wide range of temperature between −250 °C and 260 °C. This makes AA2219 the suitable candidate for aerospace applications like fabrication of cryogenic fuel tanks to store liquid oxygen and liquid hydrogen [4].

Formability is the most challenging property in the welded specimen. Once the material is welded, the strength increases but its formability is lost. Whereas, in FSW both ductility and strength are retained when compared to fusion welding [5]. The ductility is improved by increasing the heat input, which results in sound welds [6]. Strain formability tests were performed along the major strain

Foundation item: Project(ISRO/RES/3/683/15-16 dt 07.08.2015) supported by Indian Space Research Organization
Received date: 2018-07-03; **Accepted date:** 2019-01-09
Corresponding author: S MUTHUKUMARAN, PhD, Associate Professor; Tel: +91-431-2503468; E-mail: smuthu@nitt.edu; ORCID: 0000-0002- 1395-9240

direction of the friction stir welded sheets.

The result shows the improvement of formability by 20% compared to laser welded sheets [7]. Fracture initiation and growth leads to the failure of the material. It is found that the FSW joints exhibit superior fatigue crack growth resistance when compared joints welded by electron beam welding (EBM) and gas tungsten arc welding (GTAW). This is due to uniform distribution of fine precipitates with dynamically recrystallized grains in the weld region [5]. The welded specimen with a void defect fails at the weld nugget. However, the void-free samples fail at the interface of weld nugget and thermo-mechanically affected zone [8]. The formation of onion ring pattern has been described as the ring spacing of onion ring is larger at lower rotational speed than the ring spacing at higher rotational speed [9]. Onion rings are generated in the second mode by the tool pin [10]. During welding, when the probe comes in contact with the bottom plate, pulling of material occurs resulting in onion ring formation. The use of a threaded pin (with 0.067 revolutionary pitch) leads to the formation of onion rings with ascending convex and descending concave pattern at the weld interface [11]. Very few research articles have analyzed the ductility behavior and microstructure at various regions in the onion ring pattern of AA2219-T87. Hence, a detailed study has been conducted in this research work on improving the ductility of the welded material to retain the formability by changing the tool profile to enhance the metal flow. The correlation between ductility, fracture behavior and microstructure in onion ring pattern of AA2219-T87 has been explained in this article.

2 Experimental procedure

Friction stir welding of AA2219-T87 plate of 100 mm×60 mm×6 mm was carried out in butt configuration. The mechanical properties and chemical composition of AA2219-T87 are shown in Tables 1 and 2, respectively. The process parameters were selected in a wide range of traverse speed between 100 and 500 mm/min, rotational speed from 500 to 2000 r/min, and five different tool profiles such as plain cylindrical pin, cylindrical threaded pin, plain taper pin, taper threaded pin (TTP), and shoulder & taper threaded pin (STTP). The parameters were optimized to a narrow range from which eight set of experiments were carried out by varying the three parameters each at two levels. STTP and TTP tool profiles were found to be influencing weld parameters among other tool profiles for the formation of onion rings. The various weld parameters with their levels are listed in Table 3. Welding was done by the FSW machine (BiSS-ITW model), as shown in Figures 1 and 2. The tools were made of H13 tool steel material with overall length of 40 mm, diameter of 24.9 mm, tool shoulder diameter of 18 mm, tool pin length of 5.6 mm, tool pin initial diameter of 6 mm and taper end diameter of 4 mm, as shown in Figure 3. Then the welded specimens were cut as per ASTM E8 standard by wire electrical discharge machine for tensile testing. Universal testing machine (Tinius Olsen model) was used for tensile testing. The strain rate used for testing was 1 mm/min. The test results were noted to check the percentage plasticity limit before failure of the sample. The samples for metallography analysis were cut to size of 30 mm×10 mm×6 mm and cold mounted. The polished samples were etched with Kroll's reagent for macrostructure analysis and Keller's reagent for microstructure analysis. Microhardness of the welded samples was measured using Matsuzawa micro Vickers hardness

Table 1 Mechanical properties of AA2219-T87

Yield strength/ MPa	Ultimate tensile strength/MPa	Elongation/ %	Charpy impact energy/J
380	465	17.23	4.09

Table 2 AA2219-T87 chemical composition (mass fraction, %)

Copper	Manganese	Zirconium	Vanadium
5.95	0.27	0.1	0.09
Titanium	Iron	Silicon	Aluminum
0.06	0.12	0.05	Balance

Table 3 Welding parameters and their levels

Parameter	Level	
	1	2
Traverse speed/ ($mm \cdot min^{-1}$)	100	300
Rotational speed/ ($r \cdot min^{-1}$)	500	750
Tool profile	Taper threaded pin (TTP)	Shoulder and taper threaded pin (STTP)

Figure 1 Friction stir welding machine

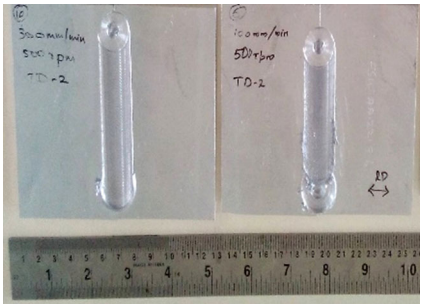

Figure 2 Welded samples

equipment (MMT-X model). The indentation load was fixed at 4.9 N for a dwell time of 15 s. The fractography analysis was carried out using Hitachi (S-3000H) scanning electron microscope equipped with electron dispersive spectroscopy (EDS) detector.

3 Results and discussion

3.1 Elongation

Melting and solidification phenomenon occurring during fusion welding process decreases the elongation and ductility thereby affecting the material formability. This short coming can be overcome by FSW [8]. The intense heat supplied and rapid cooling rates during the fusion welding process tends to generate ultra-fine grains thereby reducing the ductility of the weld specimens. For ductility retainment, heat treatment is necessary in fusion welded specimen for the attainment of microstructural changes. However, when the size of the weld specimen is too large and complex, heat treatment tends to be challenging. FSW works on the principle of plastic deformation of material before attaining recrystallization or pre-melting temperature, and hence the ductility is retained. Tool profile is found to have the maximum influence on the metal flow and ductility of the welded material. TTP tool profile and STTP tool profile have better metal flow than other tools, hence these tools are selected for welding. The tensile test results are listed in Table 4. The parameters with 100 mm/min traverse speed, 500 r/min rotational speed and STTP tool profile results maximum ductility with elongation of 86% of the base metal, followed by 81% elongation for the parameters with 100 mm/min traverse speed, 500 r/min rotational speed and TTP tool profile. When compared to GTAW, FSW has 35% increase in elongation and EBW has a 27% increase in elongation [12].

The parameters with 100 mm/min traverse speed and 500 r/min rotational speed have maximum influence on retaining ductility of the

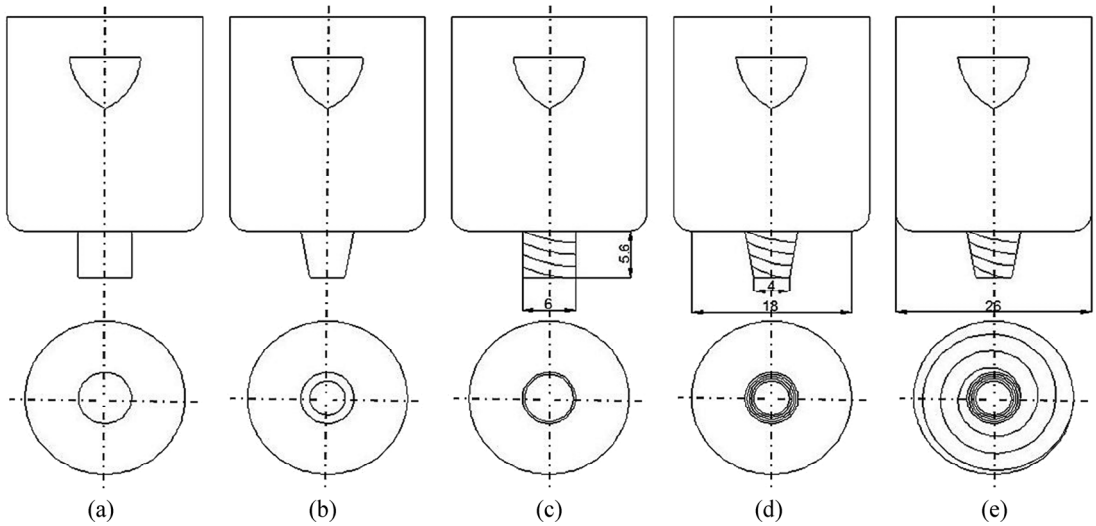

Figure 3 Various tool profile geometry: (a) Plain cylinder pin; (b) Plain taper pin; (c) Cylinder threaded pin; (d) Taper threaded pin; (e) Shoulder & taper threaded pin

Table 4 Elongation after tensile testing

Sample No.	Traverse speed/ (mm·min^{-1})	Rotational speed/ (r·min^{-1})	Tool profile	Elongation/%	Contribution/%
0	−	−	Base metal	17.23	100
1	100	500	TTP	14.00	81.25
2	300	500	TTP	11.82	63.84
3	100	750	TTP	13.89	80.61
4	300	750	TTP	13.42	77.88
5	100	500	STTP	14.89	86.41
6	300	500	STTP	11.20	65.01
7	100	750	STTP	7.57	43.93
8	300	750	STTP	12.17	70.63

material. Considering the tool profile, STTP profile yields better ductility than TTP profile. The threaded shoulder feature in STTP tool enhances the material flow which improves the ductility. This phenomenon increased ductility without compromising strength, making the joints suitable to undergo forming processes.

3.2 Tensile and yield strength

The tensile and yield strength results of the welded samples are given in Figures 4 and 5. The results of the tensile strength for different samples are in the range of 315−340 MPa. Sample 4 with parameters of 300 mm/min traverse speed, 750 r/min rotational speed and STTP pin profile exhibits maximum tensile strength.

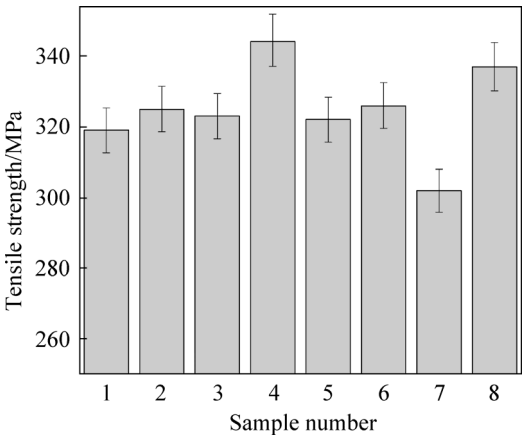

Figure 4 Tensile strength of welded samples

The yield strength varies from 145 MPa to 180 MPa. Sample 6 with 300 mm/min traverse speed, 500 r/min rotational speed and STTP pin profile has the maximum yield strength. Hence, STTP profile enhances both elongation and strength with better material flow in the weld joints.

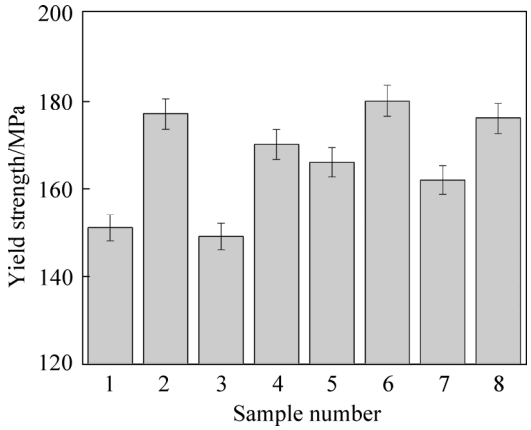

Figure 5 Yield strength of welded samples

3.3 Fracture analysis

Fracture study is performed using stereo microscope and optical microscope to identify crack initiation location [13]. The most influencing parameter for fracture growth was found to be tool profile. For TTP tool profile, all the tested tensile samples fail at the retreating side at different regions in the weld, and for STTP tool profile, all the tested tensile samples fail at the advancing side of the weld. In FSW, material flow occurs from the advancing side towards the retreating side. The role of the tool shoulder is to provide compaction for the material moved from the advancing side by the pin to the retreating side. This phenomenon is followed in weld nugget formation of TTP tool profile. The presence of a threaded profile in the tool shoulder of STTP profile aids in further material flow towards the retreating side from the advancing side in addition to the compaction provided. This phenomenon of material movement drives the STTP tool shoulder profile, which is found to be the reason for the retreating side to be stronger than the advancing side. Whereas in TTP, the retreating side

is weaker than the advancing side because compaction occurs only in the first mode by tool shoulder rather than sufficient metal transfer. In STTP profile fracture occurs at the advancing side since both pin and shoulder pull material from the advancing side towards retreating side making the advancing side weaker. In Figure 6(a), fracture initiates at the weld center and ends at the retreating side of the weld nugget; in Figure 6(b), fracture initiates at the retreating side of the nugget and propagates through it till the bottom. In Figure 6(c), fracture initiates at the retreating side of TMAZ and runs through TMAZ till the bottom. In Figure 6(d), fracture initiates at the retreating side of TMAZ and passes through the weld. Hence TMAZ is the weakest zone for 750 r/min, due to the onion ring formation at the weld nugget which increases the strength of the weld nugget. Whereas in Figures 7(a) and (b) with STTP profile, the fractures initiate at advancing side of the weld and propagate towards the retreating side. In Figures 7(c) and (d), fractures initiate at HAZ of advancing side and propagate towards the welded bottom. This relation shows that TTP tool profile provides stronger advancing side and STTP tool profile provides strong retreating side due to material flow. The microstructures of the start and end of the fracture zone at both 500 and 750 r/min are shown in Figures 8 and 9.

They confirm that the fracture at 500 r/min begins at weld nugget and ends at the weld nugget,

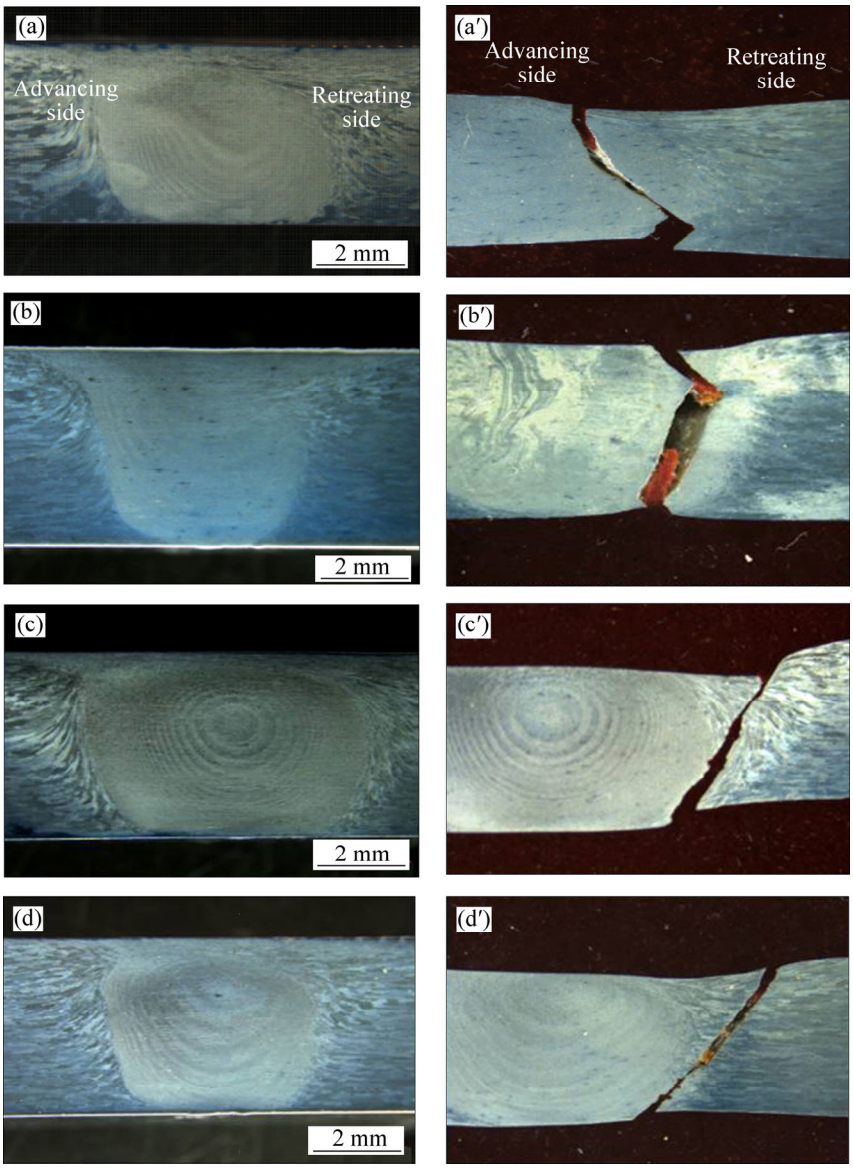

Figure 6 Macrostructures of weldment (a−d) and fracture location of welded joints (a′−d′) for TTP tool profile: (a, a′) 100 mm/min, 500 r/min; (b, b′) 300 mm/min, 500 r/min, TTP; (c, c′) 100 mm/min, 750 r/min, TTP; (d, d′) 300 mm/min, 750 r/min, TTP

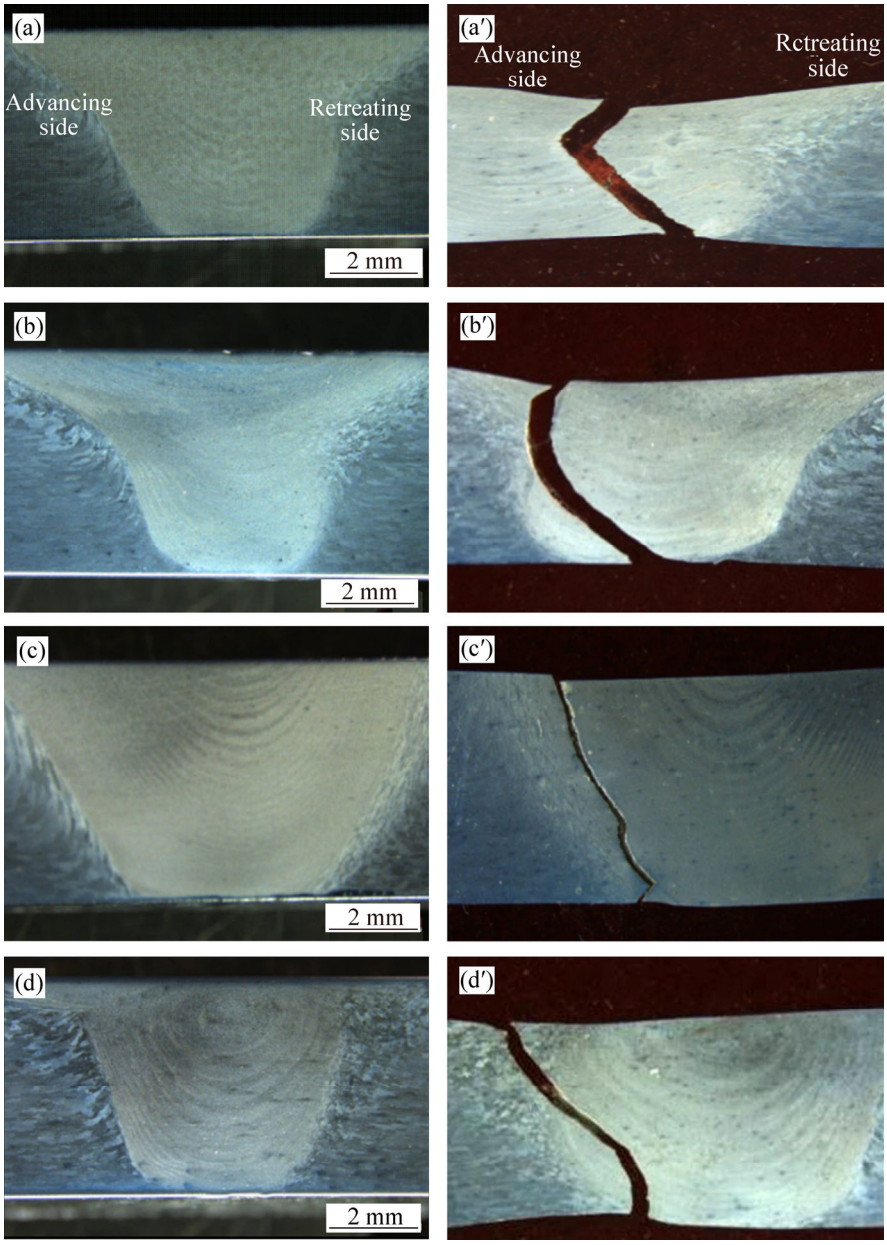

Figure 7 Macrostructures of weldment (a−d) and fracture locations of welded joints (a′−d′) for STTP tool profile: (a, a′) 100 mm/min, 500 r/min, STTP; (b, b′) 300 mm/min, 500 r/min, STTP; (c, c′) 100 mm/min, 750 r/min, STTP; (d, d′) 300 mm/min, 750 r/min, STTP

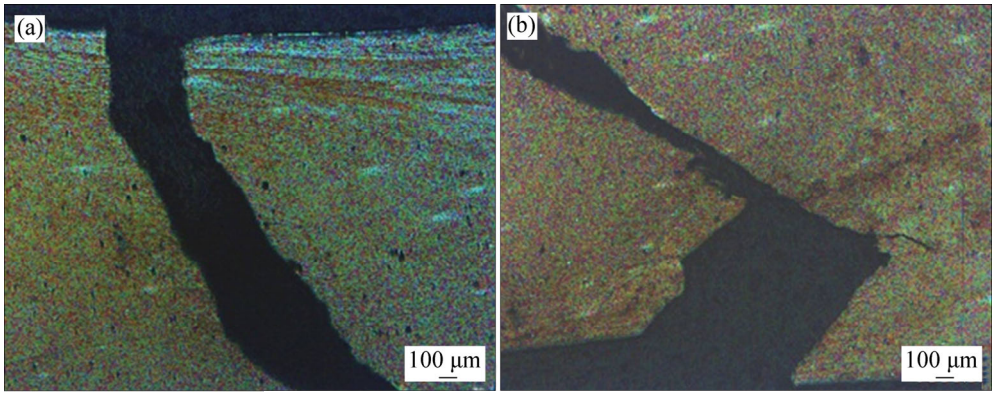

Figure 8 Fracture path for 500 r/min: (a) Fracture propagation in first mode of weld; (b) Fracture propagation in second mode of weld

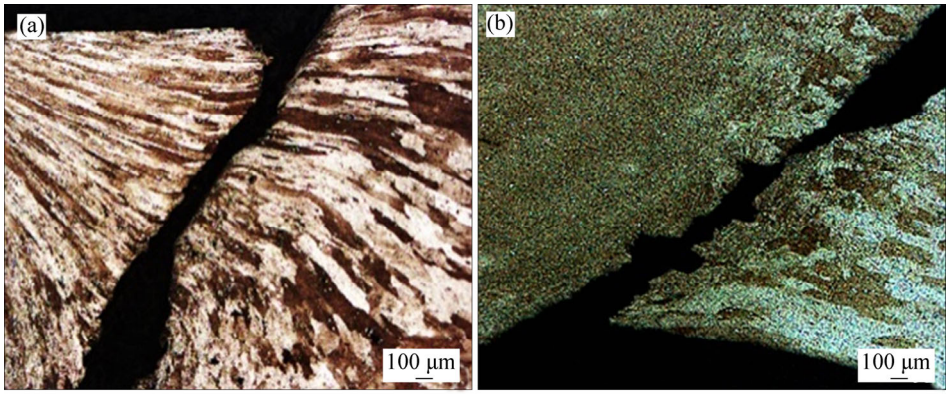

Figure 9 Fracture path for 750 r/min: (a) Fracture propagation in first mode of weld; (b) Fracture propagation in second mode of weld

which increases the fracture toughness of the nugget zone. Therefore, the failure of the welds has shifted to nugget. The fracture at 750 r/min, starts at TMAZ and ends at TMAZ. The onion ring material flow was fragile compared to the nugget zone.

3.4 Microstructure of onion ring

The macrostructures of the welded sample with traverse speed of 300 mm/min, rotational speed of 750 r/min and STTP tool profile reveal onion ring pattern shown in Figure 10(a), where the advancing side, retreating side and weld nugget are clearly visible with onion ring pattern formed. It is found that the material at the retreating side does not enter the advancing side, but the material at the advancing side enters the retreating side of the weld. The formation of flash has been reported to occur due to the piling up of the top surface material at the retreating side [14]. Figure 10(b) shows the top portion adjacent to the core of the onion ring which has a mixture of finer and coarser grains. Figure 10(c) shows the core of the onion ring occuping coarser grains. Figure 10(d) shows the microstructure of center and the bottom portion of onion ring which has coarser grains followed by finer grains. Figure 10(e) reveals the next layer of the onion ring which is ultra-fine structured. On moving from top surface to root of the weld nugget, the grain size decreases [15]. The formation of onion ring pattern in stir zone results in fluctuation of hardness. The onion ring formation increases the tensile properties in the longitudinal direction of the stir zone [16]. Figure 10(b) shows an average grain size of 10 μm whereas Figure 10(c) reveals coarser grains with an average grain size of 13 μm. The center portion of the weld nugget cross section has fine grains with an average grain size of 6 μm in Figures 10(d), and in Figure 10(e) the bottom portion of the weld nugget is found to have ultra-fine grains with an average grain size of 4 μm.

3.5 Fractography

The SEM image of the fracture surface shown in Figure 11(a) corresponds to the parameters 500 r/min rotational speed, 100 mm/min traverse speed and STTP tool profile. Figure 11(b) represents the fracture surface of the parameters 500 r/min rotational speed, 100 mm/min traverse speed and TTP tool profile. This comparative analysis explains the failure pattern by dimples in the fracture surface indicating the ductile mode of fracture [13]. The orderly arrangement of grains during the stirring action of the tool increases the ductility of the weldment.

3.6 Microhardness distribution

Microhardness of the welded samples is measured using Vickers hardness scale at four different layers of the welded specimen, namely 1.0, 2.5, 4.0 and 5.0 mm, respectively making 25 indentations at each layer from top surface at an interval of 1 mm in horizonal direction along the different regions of the welded zone, as shown in Figure 12.

The hardness value measured at different regions are represented in Table 5. The weakest zone of the weld was at 4 mm (hardness value of HV 86) from the top surface where the crack runs through. The overall hardness value shows that TMAZ and HAZ are weaker than the weld nugget due to the strengthening of the weld nugget by the formation of onion ring pattern.

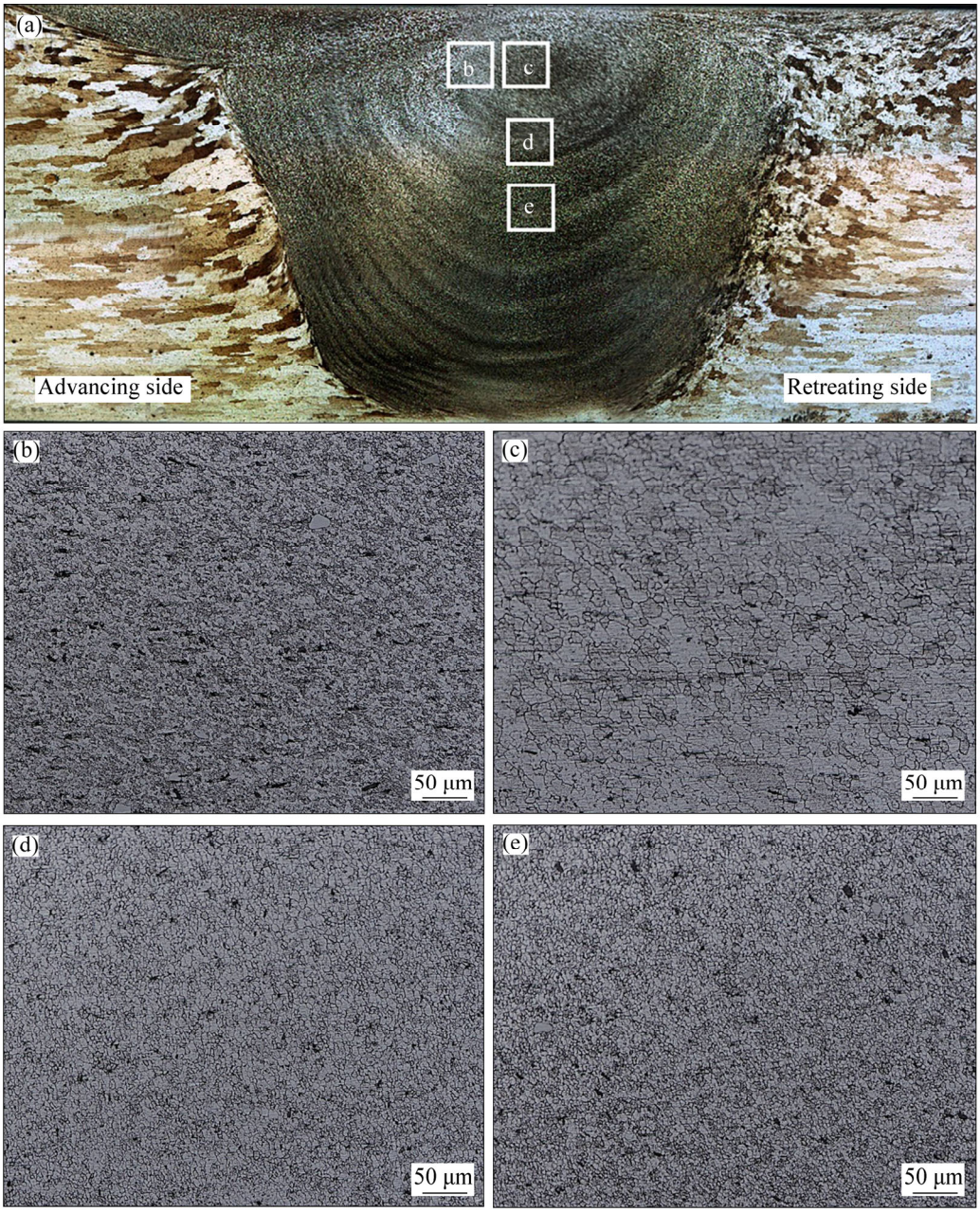

Figure 10 Macrostructure and microstructure of onion ring pattern: (a) Macrostructure of weld nugget; (b) Advancing side of weld nugget; (c) Centre of onion ring; (d) Third layer of onion ring; (d) Fifth layer of onion ring

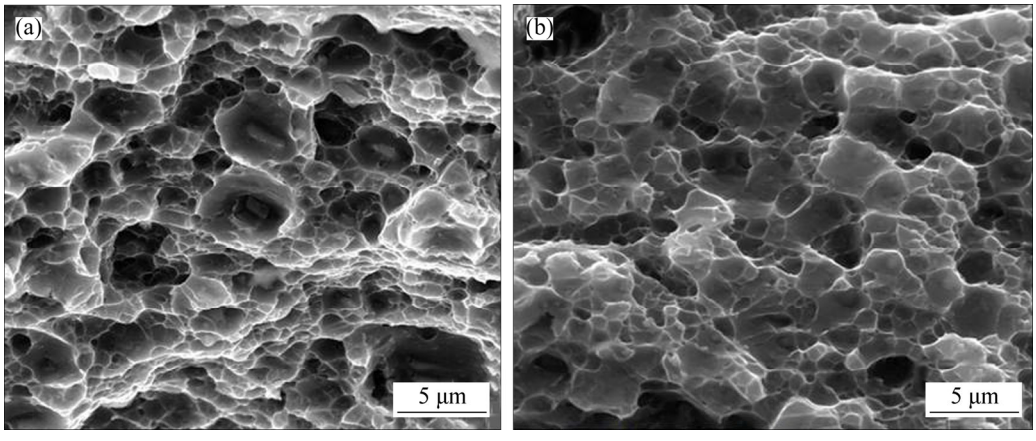

Figure 11 SEM images of fracture surface: (a) 100 mm/min, 500 r/min and STTP; (b) 500 r/min, 100 mm/min and TTP

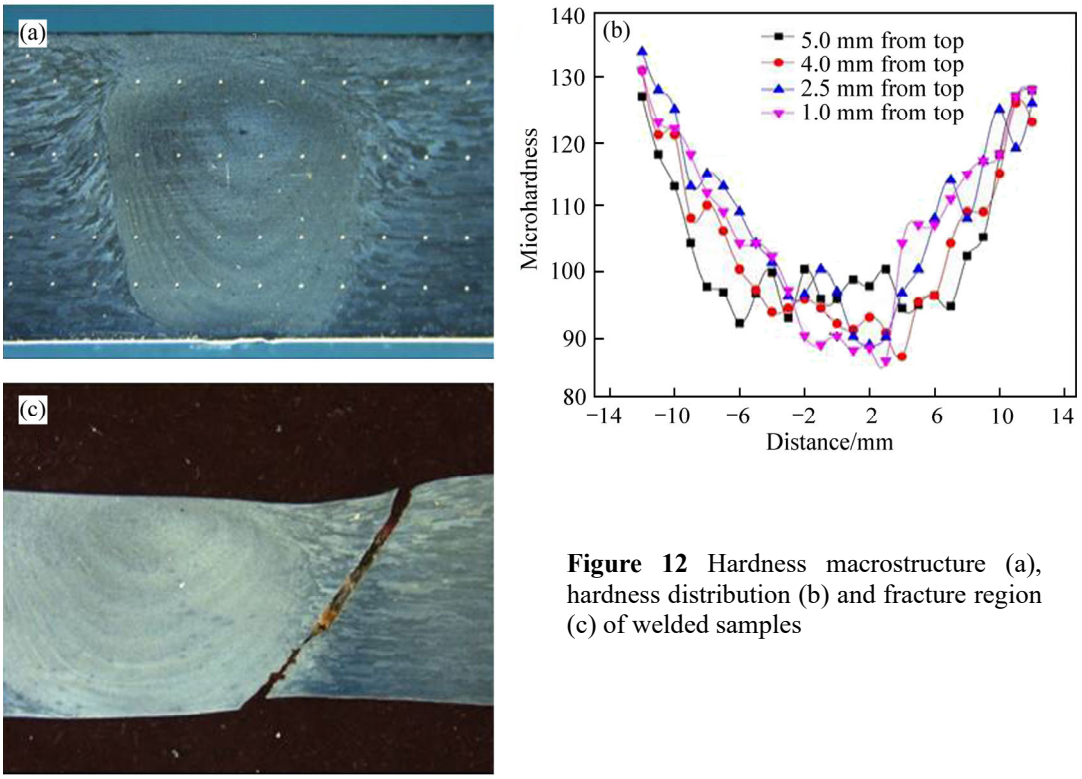

Figure 12 Hardness macrostructure (a), hardness distribution (b) and fracture region (c) of welded samples

Table 5 Microhardness distribution along weld cross section

Distance from top/mm	Microhardness (HV)											
	−12 mm	−11 mm	−10 mm	−9 mm	−8 mm	−7 mm	−6 mm	−5 mm	−4 mm	−3 mm	−2 mm	−1 mm
5.0	127	118	113	104	97.3	96.4	91.9	96.2	99.5	92.4	100	95.4
4.0	131	121	121	108	110	106	100	96.8	93.3	93.9	95.3	93.9
2.5	134	128	125	113	115	113	109	104	101	95.8	96.1	100
1.0	131	123	122	118	112	109	104	104	102	96.7	89.7	88.3
Distance from top/mm	Microhardness (HV)											
	0	1 mm	2 mm	3 mm	4 mm	5 mm	6 mm	7 mm	8 mm	9 mm	10 mm	11 mm	12 mm
5.0	95.4	98.4	97.4	100	93.9	94.4	95.9	94.2	102	105	118	127	128
4.0	91.5	90.6	92.5	90.1	86.4	94.9	95.9	104	109	109	115	126	123
2.5	96.5	89.6	88.3	89.5	96.3	100	108	114	108	117	125	119	126
1.0	89.6	87.4	87.8	85.7	104	107	107	111	115	117	118	127	128

4 Conclusions

In this work, the AA2219-T87 material is welded successfully by FSW to improve the ductility which helps in improving the formability of welded components. The following conclusions are arrived.

1) STTP tool profile yields higher ductility in 500 r/min tool rotational speed and 100 mm/min traverse speed combination. This combination improves the material flow and grain refinement resulting in the maximum elongation of 86.41% of the base material. STTP also has better tensile property than TTP tool profile.

2) In TTP tool profile, failure occurs at the retreating side and for STTP tool profile failure occurs at the advancing side of the weld.

3) The onion ring pattern increases the strength of the weld nugget. Hence, the failure of the welded sample occurs at TMAZ and HAZ.

4) The fracture occurs at lower hardness area like TMAZ and HAZ, which is confirmed by microhardness distribution across the different

zones of the welded joint. Higher hardness at the weld nugget zone and comparatively lower hardness have been reported at other zones.

References

[1] ARTHUR C, MARSHALL N. Metal flow in friction stir welding [R]. NASA Marshal Space Flight Centre, 2017.

[2] HASAN M M, ISHAK M, REJAB M R M. Effect of backing material and clamping system on the tensile strength of dissimilar AA7075-AA2024 friction stir welds [J]. International Journal of Advanced Manufacturing Technology, 2017, 91(9−12): 3991−4007.

[3] MUTHUKUMARAN S, MUKHERJEE S K. Two modes of metal flow phenomenon in friction stir welding process [J] Science and Technology of Welding and Joining, 2006, 11(3): 337−340. DOI: http://www.tandfonline.com/doi/full/10.1179/1743 29306X107665.

[4] ARORA K S, PANDEY S, SCHAPER M, KUMAR R. Microstructure evolution during friction stir welding of aluminum alloy AA2219 [J]. Journal of Materials Science and Technology, 2010, 26(8): 747−753. DOI: http://dx.doi.org/10.1016/S1005-0302(10)60118-1.

[5] MALARVIZHI S, BALASUBRAMANIAN V. Fatigue crack growth resistance of gas tungsten arc, electron beam and friction stir welded joints of AA2219 aluminium alloy [J] Materials and Design, 2011, 32(3): 1205−1214.

[6] KOLAHGAR S, GHAFFARPOUR M, HABIBI N, KOKABI A H, AKBARZADEH A. Formability of friction stir-welded blanks with different thickness ratios [J]. Metallurgical and Materials Transactions A: Physical Metallurgy and Materials Science, 2016, 47(5): 2177−2187.

[7] MILES M P, PEW J, NELSON T W, LI M. Comparison of formability of friction stir welded and laser welded dual phase 590 steel sheets [J]. Science and Technology of Welding and Joining, 2006, 11(4): 384−388. DOI: http://www.tandfonline.com/doi/full/10.1179/174329306X107737.

[8] LIU H J, FUJII H, MAEDA M, NOGI K. Tensile properties and fracture locations of friction-stir-welded joints of 2017-T351 aluminum alloy [J]. Journal of Materials Processing Technology, 2003, 142(3): 692−696.

[9] KRISHNAN K N. On the formation of onion rings in friction stir welds [J]. Materials Science and Engineering A, 2002, 327(2): 246−251.

[10] MUTHUKUMARAN S, MUKHERJEE S K. Multi-layered metal flow and formation of onion rings in friction stir welds [J]. International Journal of Advanced Manufacturing Technology, 2008, 38(1, 2): 68−73.

[11] YOON T J, YUN J G, KANG C Y. Formation mechanism of typical onion ring structures and void defects in friction stir lap welded dissimilar aluminum alloys [J]. Materials and Design, 2016, 90: 568−578. DOI: http://dx.doi.org/10.1016/j.matdes.2015.11.014.

[12] MILLERS M P, DECKER B J, NELSON T W. Formability and strength of friction-stir-welded aluminum sheets [J]. Metallurgical and Materials Transactions A, 2004, 35: 3461−3468.

[13] MAGGIOLINI E, TOVO R, SUSMEL L, JAMES M N, HATTINGH D G. Crack path and fracture analysis in FSW of small diameter 6082-T6 aluminium tubes under tension–torsion loading [J]. International Journal of Fatigue, 2016, 92: 478−487. DOI: http://dx.doi.org/10.1016/j.ijfatigue.2016. 02.043.

[14] ZHANG Z, ZHANG H W. Numerical studies on controlling of process parameters in friction stir welding [J]. Journal of Materials Processing Technology, 2009, 209(1): 241−270.

[15] ZHANG Z, HU C P, WU Q. Three dimensional Monte Carlo simulation of grain growth in friction stir welding [J]. Journal of Plasticity Engineering, 2017, 24(3): 1287−1296.

[16] KHODIR S A, SHIBAYANAGI T. Friction stir welding of dissimilar AA2024 and AA7075 aluminum alloys [J]. Materials Science and Engineering B: Solid-State Materials for Advanced Technology, 2008, 148(1−3): 82−87.

(Edited by FANG Jing-hua)

中文导读

焊接参数对搅拌摩擦焊接 AA2219-T87 材料韧性、洋葱圆环的断裂行为的影响

摘要：与熔焊相比，搅拌摩擦焊可以更好地保持材料的韧性和塑性，提高焊接的抗裂稳定性。本研究旨在提高焊接接头的延性和强度。刀具廓形在保持延性、分析金属流动行为和确定断裂起始点等方面起着重要作用。分析了洋葱圆环不同区域的微观结构，得出了洋葱圆环强度与金属流型的关系。结果表明，洋葱圆环强化了焊缝熔核。肩部和锥形螺纹型线刀具具有优异的力学性能。显微硬度数据表明，断口经过热影响区和热机械影响区等低硬度区。扫描电镜图像显示了细长的晶粒和韧窝，证实了断裂为韧性断裂。

关键词：塑性；金属流动；洋葱圆环；断裂；搅拌摩擦焊接